Inorganica Chimica Acta 420 (2014) 39–46

Contents lists available at ScienceDirect

Inorganica Chimica Acta

journal homepage: www.elsevier.com/locate/ica

New metal complexes of NNO tridentate ligands: Effect of metal center and co-ligand on biological activity

I. Machado [a], M. Fernández [a], L. Becco [b], B. Garat [b], R.F. Brissos [c], N. Zabarska [c], P. Gamez [c,d], F. Marques [e], I. Correia [f], J. Costa Pessoa [f], D. Gambino [a,*]

[a] Química Inorgánica, DEC, Facultad de Química, Universidad de la República, Gral. Flores 2124, 11800 Montevideo, Uruguay
[b] Laboratorio de Interacciones Moleculares, Facultad de Ciencias, Universidad de la República, Iguá 4225, 11400 Montevideo, Uruguay
[c] Departament de Química Inorgánica, QBI, Universitat de Barcelona, Martí i Franquès 1-11, 08028 Barcelona, Spain
[d] Institució Catalana de Recerca i Estudis Avançats (ICREA), Passeig Lluís Companys 23, 08010 Barcelona, Spain
[e] Unidade de Ciências Químicas e Radiofarmacêuticas, Instituto Superior Técnico, Campus Tecnológico e Nuclear, Estrada Nacional 10, 2695-066 Bobadela LRS Sacavém, Portugal
[f] Centro de Química Estrutural, Instituto Superior Técnico, Universidade Técnica de Lisboa, Av Rovisco Pais, 1049-001 Lisboa, Portugal

ARTICLE INFO

Article history:
Available online 8 November 2013

Recent Advances in Vanadium Chemistry
Special Issue

Keywords:
Oxidovanadium(IV) and dioxidovanadium(V) complexes
Gallium(III)
N,N,O ligands
Antitrypanosomal
Antitumoral

ABSTRACT

In the search for new agents against *Trypanosoma cruzi* and cancer the effect of the nature of the metal center and of the presence of a polypiridyl coligand on the antitrypanosomal and antitumoral activities of selected N,N,O ligands [2-(benzothiazol-2-yl-hydrazonomethyl phenol (HL1) and 2-(benzothiazol-2-yl-hydrazonomethyl)-6-methoxyphenol (HL2)] is explored. The new complexes $[V^{V}O_2(L1)]$, $[V^{V}O_2(L2)]$, $[V^{IV}O(L1\text{-}H)(phen))]$ and $[Ga^{III}(L2)_2](NO_3)$ were synthesized and characterized by using different techniques. The stability of the vanadium complexes in solution was investigated by EPR and ^{51}V NMR spectroscopies and that of the gallium compound by UV–Vis spectroscopy, ^{1}H NMR and conductivity measurements. While the vanadium complexes show high stability in DMSO, the gallium complex shows very good stability in DMSO and moderate stability in aqueous – DMSO medium.

The cytotoxicity on human tumor cell lines (ovarian A2780, breast MCF7 and prostate PC3 cell lines) that show different sensitivity to cisplatin was evaluated. All the compounds evidenced antiproliferative activity in the micromolar range. The highest cytotoxic activity, in molar units, is shown by $[Ga^{III}(L2)_2](NO_3)$ (IC_{50}: 1.7 μM) and $[V^{IV}O(L1\text{-}H)(phen)]$ (IC_{50}: 2.7 μM) against the ovarian cancer cells. With the exception of $[V^{V}O_2(L1)]$, the cytotoxic activity of the ligands and complexes is similar to that of cisplatin in A2780 cells and surpass cisplatin in the other tumor cells. Regarding the activity on *T. cruzi*, $[V^{IV}O(L1\text{-}H)(phen)]$ showed a 10-fold decrease of IC_{50} with respect to HL1 and an IC_{50} value (10.7 μM) in the same order of that of the antitrypanosomal drug Nifurtimox (IC_{50}: 6.0 μM). HL2 showed significant growth inhibitory effect on the parasite (IC_{50}: 23.5 μM) and its coordination to Ga(III) lead to a 2-fold increase in activity in molar units (IC_{50}: 14.2 μM). In order to explain the high inhibitory activity of $[V^{IV}O(L1\text{-}H)(phen)]$ against the parasite and the tumor cells, the interaction of this compound with plasmid DNA was preliminarily evaluated by AFM. The corresponding images suggest that DNA may be considered as a potential target.

1. Introduction

Cancer is the second largest cause of death in developed countries and the World Health Organization has predicted that the number of worldwide deaths from cancer will rise to over 13.1 million people in 2030 [1]. Although cisplatin and related Pt complexes still remain the most extensively used anticancer drugs, their high toxicity, incidence of resistance to treatment and lack of response on some tumor types severely reduce their clinical value. Extensive research in the quest for anticancer drugs bearing improved therapeutic indexes and wider activity spectra has led to the development of novel metal-based compounds that show interesting antitumor activities [2–8]. In particular, the antineoplastic activity of simple Ga(III) salts was discovered in the 1970s and much work has been done since then to elucidate their mechanism of action. To prevent hydrolysis processes and to improve cell membrane permeation and oral bioavailability, Ga(III) coordination compounds are currently being developed. So far, tris(8-quinolato)gallium(III) and tris(maltolato)gallium(III) have entered the clinical trial phases and are being evaluated as potential oral antitumoral agents [9–14]. On the other hand, research efforts on the medicinal chemistry of vanadium have also partially focused on developing potential anticancer compounds. Hence, different

* Corresponding author. Tel.: +598 29249739; fax: +598 29241906.
E-mail address: dgambino@fq.edu.uy (D. Gambino).

0020-1693/$ - see front matter © 2013 Elsevier B.V. All rights reserved.
http://dx.doi.org/10.1016/j.ica.2013.10.022

vanadium compounds have shown interesting antitumoral properties [15–18].

American trypanosomiasis or Chagas disease (etiologic agent: *Trypanosoma cruzi*) is endemic of Latin America where it affects around 10 million people and causes more deaths than any other parasitic disease. In recent years, globalization and immigration have also led to the appearance of several infection cases in developed countries [19,20]. The treatment of Chagas disease is still based on old and quite unspecific nitroheterocyclic drugs, nifurtimox and benznidazole, that have significant activity only in the acute phase of the disease and give rise to severe side effects. Therefore, the development of more efficacious and less toxic drugs, that could also circumvent emerging drug resistance, is urgently needed [21]. During the last decades, inorganic medicinal chemists have demonstrated that the design of bioactive metal-based compounds is a promising approach for the development of new drugs against this disease [22–28].

In the search for new treatments against tropical diseases caused by trypanosomatid parasites (*T. cruzi*, *Trypanosoma brucei*, *Leishmania* spp) and against cancer, different series of oxidovanadium(IV), dioxidovanadium(V) and gallium(III) compounds have been developed by us as prospective anti-*T. cruzi* and/or anticancer agents [23,30–34]. Highly-proliferative cells such as trypanosomatid parasites and tumor cells show metabolic similarities that lead in many cases to a correlation between antitrypanosomal and antitumor activities. For instance, some compounds that efficiently interact with DNA also exert antitrypanosomal activity [23,28,29]. Having this fact in mind, we explored both activities for different series of metal compounds [30,35–39].

Coordination to metal ions may lead to important changes in bioavailability and bioactivity of organic compounds that in turn could promote desirable improvement in their overall biological behavior. In fact, the biological behavior of metal-based compounds is determined not only by the nature of the bioactive ligand but also by the nature and oxidation state of the metal centre and the electronic and physicochemical properties of the whole complex that is highly dependent on the presence of coligands. The modification of each of these features would allow the fine-tuning of important biological properties.

To explore the effect of the nature of the metal center and of the presence of certain coligands on the antitrypanosomal and antitumoral activities of selected N,N,O ligands, we currently synthesized new dioxidovanadium(V), oxidovanadium(IV) and gallium(III) complexes of the ligands shown in Fig. 1. The compounds were designed, prepared and characterized in the solid state and in solution. The nature of the complexes in solution, as well as their stability with time was investigated. The biological activity of the compounds was explored by evaluating their cytotoxicity on three human tumor cell lines that show different sensitivity to cisplatin and their growth inhibitory effect on the epimastigote life cycle form of *T. cruzi*. Furthermore, DNA was preliminarly evaluated as a possible target by using atomic force microscopy (AFM) for one of the most active compounds having a DNA intercalating ligand in the oxidovanadium(IV) coordination sphere.

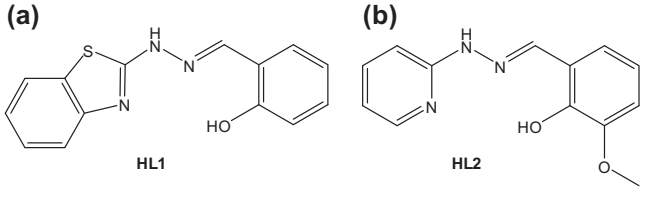

Fig. 1. Selected N,N,O ligands: (a) 2-(benzothiazol-2-yl-hydrazonomethyl phenol (HL1); (b) 2-(benzothiazol-2-yl-hydrazonomethyl)-6-methoxyphenol (HL2).

2. Experimental

2.1. Materials

All common laboratory chemicals were purchased from commercial sources and used without further purification. The N,N,O ligands HL1 and HL2 are Schiff bases synthesized by condensation of the corresponding aldehyde and hydrazine in an equimolar mixture as previously described [40–43].

HL1. ^{1}H NMR: δ = 12.20 (s, 1H), 10.40 (s br, 1H), 8.46 (s, 1H), 7.77 (d, 1H), 7.64 (d, 1H), 7.29 (m, 3H),7.12 (t, 1H), 6.93 (m, 2H) ppm.

HL2. ^{1}H NMR: δ = 10.92 (s, 1H), 9.96 (s, 1H), 8.30 (s, 1H), 8.13 (d, 1H),7.65 (m, 1H), 7.22 (d, 2H), 7.07 (d, 1H), 6.95 (d, 1H), 6.78 (m, 1H), 6.77 (m, 1H), 3.80 (s, 3H) ppm.

2.2. Syntheses of the complexes

2.2.1. Synthesis of the dioxidovanadium(V) complexes, [V^VO_2(L)], **1–2**

The new [V^VO_2(L)] complexes, where L = 2-(benzothiazol-2-yl-hydrazonomethyl)phenolate (L1) or 2-(benzothiazol-2-yl-hydrazonomethyl)-6-methoxyphenolate (L2), were prepared by mixing [$V^{IV}O$(acac)$_2$] (0.188 mmol, 50 mg, acac = acetylacetonate) with HL (0.188 mmol, 53 mg HL1, 46 mg HL2) in methanol (10 mL) and then keeping the mixture for 20 h under reflux. In each case, the greenish solid was isolated by centrifugation and washed with two 2 mL portions of MeOH.

[V^VO_2(L1)], **1**. Yield: 17 mg, 39%. *Anal.* (%) Calc. for $C_{14}H_{10}N_3O_3$SV: C, 47.87; H, 2.87; N, 11.96; S, 9.13. Found: C, 47.44; H, 2.89, N, 11.90; S, 9.02. Λ_M(DMSO): 8.0 Scm^{2}mol^{-1}. ^{1}H NMR: δ = 8.68 (s, 1H), 7.78 (m, 1H), 7.53 (d, 1H), 7.35 (d, 1H),7.28 (m, 2H), 7.03 (t, 1H), 6.80 (m, 2H) ppm.

[V^VO_2(L2)], *2* Yield: 51 mg, 84%. *Anal.* (%) Calc. for $C_{13}H_{12}N_3O_4V$: C, 48.01; H, 3.72; N, 12.92. Found: C, 48.18; H, 3.67, N, 12.88. Λ_M(-DMSO): 7.0 Scm^2 mol^{-1}. ^{1}H NMR: δ = 8.57 (s, 1H), 8.18 (s, 1H), 7.69 (d, 1H), 7.22, 7.13, 7.01, 6.88, 6.79, 6.67 (m, 6H), 3.77 (s, 3H) ppm.

2.2.2. Synthesis of [$V^{IV}O$(L1-H)(phen))], **3**

[$V^{IV}O$(L1-H)(phen)] was synthesized by the following procedure: 0.375 mmol (91 mg) of HL1 and 0.375 mmol of phen (74 mg) were suspended in 15 mL of ethanol previously purged with nitrogen for 10 min. [$V^{IV}O$(acac)$_2$] (0.375 mmol, 100 mg) was suspended in 5 mL of ethanol, previously purged with nitrogen, and was added to the previous mixture. This solution was then refluxed under nitrogen for 24 h. The brown–red solid formed was filtered off from the hot mixture, and then washed three times with 2 mL portions of EtOH:Et$_2$O (1:1).

[$V^{IV}O$(L1-H)(phen)], **3.** Yield: 80 mg, 41%. *Anal.* Calc. for $C_{26}H_{17}N_5O_2$SV: C, 60.70; H, 3.33; N, 13.61; S, 6.23. Found: C, 60.31; H, 3.53; N, 13.36; S, 6.10. ESI-MS (electrospray ionization mass spectra, positive mode) (MeOH) *m/z* [Found (Calc.)]: 515.0 (514.05) (90%) (VOphenL1$^+$), 536.9 (537.04) (45%) (VOphenL1Na$^+$), 552.9 (553.02) (20%) (VOphenL1K$^+$). Λ_M(DMSO): 5.0 Scm^2 mol^{-1}.

2.2.3. Synthesis of the [Ga(L2)$_2$](NO$_3$), **4**

[Ga^{III}(L2)$_2$](NO$_3$) was synthesized by reaction of 0.141 mmol (57 mg) of Ga(NO$_3$)$_3$ 8.15 H$_2$O with 0.282 mmol (68 mg) of HL2, each reactant previously dissolved in 2 and 8 mL of methanol, respectively. The reaction mixture was stirred during 16 h at room temperature. A yellow solid precipitated and was isolated by centrifugation and washed twice with 1 mL portions of MeOH.

[Ga^{III}(L2)$_2$](NO$_3$), **4**. Yield: 42 mg, 48%. *Anal.* (%) Calc. for $C_{26}H_{24}N_7O_7$Ga: C, 50.68; H, 3.93; N, 15.91. Found: C, 50.82; H, 3.84; N, 15.65. Λ_M(DMSO): 29.8 Scm^2 mol^{-1}. ^{1}H NMR: δ = 12.74 (s, 1H), 8.64 (s, 1H), 7.81 (m, 1H), 7.74 (d, 1H), 7.02 (m, 2H), 6.86 (m,

2H), 6.62 (dd, 1H), 3.49 (s, 3H) ppm. λ_{max} (buffer PBS pH 7.0-DMSO 50:50 v/v) ($\varepsilon M^{-1}\,cm^{-1}$): 459 ($9.69 \times 10^3$), 440 ($9.75 \times 10^3$), 334 ($3.06 \times 10^4$), 250 ($1.84 \times 10^4$) nm.

2.3. Physicochemical characterization

C, H, N and S analyses were carried out with a Carlo Erba Model EA1108 elemental analyzer. Conductimetric measurements were done at 25 °C in 10^{-3} M dimethylsulfoxide (DMSO) solutions using a Conductivity Meter 4310 Jenway [44]. A 500-MS Varian Ion Trap Mass Spectrometer was used to record the electrospray ionization mass spectra (ESI-MS) of methanol solutions of the complexes in the positive mode; the complexes were first dissolved in a minimum amount of DMF and then diluted with MeOH. Each spectrum was obtained as a combination of several scans for each sample. The UV–Vis absorption spectra were measured with a Shimadzu UV-1603 spectrophotometer. The FTIR absorption spectra (4000–400 cm^{-1}) of the complexes and the free ligands were measured as KBr pellets with a Bomen FTIR model M102 instrument. ^1H NMR spectra of the free ligands and of the complexes were recorded on a Bruker DPX-400 instrument (at 400 MHz). Experiments were carried out at 30 °C in DMSO-d_6. COSY experiments were performed with the same instrument.

^{51}V NMR spectra of *ca.* 3 mM solutions of the complexes in DMSO and DMF (p.a. grade) (5% D_2O was added) were recorded on a Bruker Avance III 400 MHz instrument immediately after dissolution, and after a week standing in aerobic conditions at room temperature. ^{51}V chemical shifts were referenced relative to neat V^VOCl_3 as external standard. EPR spectra were recorded at 77 K with a Bruker ESP 300E X-band spectrometer coupled to a Bruker ER041 X-band frequency meter (9.45 GHz). The complexes were dissolved at room temperature in DMSO or DMF (p.a. grade), previously degassed with N_2 for 10 min, and the obtained solutions were then frozen in liquid nitrogen. The spin Hamiltonian parameters were obtained by simulation of the spectra with the computer program of Rockenbauer and Korecz [45].

2.4. Biological activity

2.4.1. Cell viability assays in human tumor cell lines

The ovarian A2780, breast MCF7 and prostate PC3 human carcinoma cell lines (ATCC) were cultured in media (Gibco) RPMI 1640 (A2780, PC3) or DMEM containing GlutaMax I (MCF7) supplemented with 10% FBS and 1% antibiotics at 37 °C in a 5% CO_2 humidified atmosphere (Heraeus, Germany). The cells were adherent in monolayers and, when confluent, were dislodged by a 0.05% trypsin–EDTA solution (Gibco). Cell viability was evaluated by the colorimetric MTT assay, which measures the reduction of yellow 3-(4,5-dimethylthiazol-2-yl)-2,5-diphenyltetrazolium bromide (MTT) to an insoluble, purple formazan product by metabolically active cells [46]. For this purpose, cells were seeded in 200 μL aliquots of complete RPMI or DMEM media into 96-well plates. The cell densities were 8×10^3 (A2780, PC3) and 1×10^4 (MCF7) viable cells per well chosen to ensure exponential growth of untreated control samples throughout the experiment. Cells were allowed to settle for 24 h followed by the addition of dilution series of the test compounds in fresh medium (200 μL/well). Compounds were first solubilized in DMSO and then in medium, and added to final concentrations from 0.1 μM to 200 μM. The final concentration of DMSO in medium did not exceed 1%. For comparison the cytotoxicity of cisplatin (the reference positive control for the A2780 cells) was evaluated under the same experimental conditions. In this way, cisplatin was first solubilized in water and then added at the same concentration range. Following continuous exposure to the compounds for 72 h, 37 °C/5% CO_2 the medium was replaced by 200 μL MTT solution (0.5 mg/mL PBS). After 3 h incubation, MTT solution was discarded, and the formazan product formed by viable cells was dissolved in DMSO (200 μL/ well). The cellular viability was evaluated by measuring the absorbance at 570 nm using a plate spectrophotometer (PowerWave Xs, Bio-tek Instruments, VT, USA). Based on nonlinear regression analysis of dose *vs.* response data (GRAPHPAD PRISM software), the cytotoxic effects of the compounds were quantified calculating the drug concentration inhibiting tumor cell growth by 50% (IC_{50}). Evaluation was based on at least two independent experiments, each comprising eight replicates per concentration [14].

2.4.2. In vitro anti-trypanosoma cruzi activity

T. cruzi epimastigotes of the Dm28c strain were maintained in exponential growth at 28 °C in liver infusion tryptose (LIT) medium complemented with 10% (v/v) fetal calf serum (FCS). The effect on cell growth was analyzed incubating an initial concentration of 1×10^6 cells/mL with various concentrations of the compounds for 5 days. Compounds were added as stock DMSO solutions immediately after the preparation of these solutions. The percentage of cell growth was followed by measuring the absorbance, A, of the culture at 595 nm (A_{595}) and calculated as follows:% = $(Ap - A_0p)/(Ac - A_0c) \times 100$, where $Ap = A_{595}$ of the culture containing the drug at day 5; $A_0p = A_{595}$ of the culture containing the drug at day 0; $Ac = A_{595}$ of the culture in the absence of any drug (control) at day 5; $A_0c = A_{595}$ in the absence of the drug at day 0. The results are presented as averages ± SD (standard deviation). The final DMSO concentration in the culture media never exceeded 0.4% (v/v) and had no effect by itself on the proliferation of the parasites [30]. Nifurtimox (Nfx) was used as the reference trypanosomicidal drug. Dose–response curves were recorded and the IC_{50} values (50% inhibitory concentration) were determined.

2.5. Atomic force microscopy (AFM) studies

To optimize the observation of the conformational changes in the tertiary structure of pBR322 plasmid DNA, it was heated at 60 °C for 30 min to obtain a majority of open circular form. 15 ng of pBR322 DNA were incubated in an appropriate volume with the required compound concentration corresponding to the molar ratio base pairs (bp):compound 5:1. Each $V^{IV}O$-complex was dissolved in a minimal amount of DMSO, and (4-(2-hydroxyethyl)-1-piperazineethanesulfonic acid buffer (HEPES) pH 7.4 was then added up to the required concentration. The different solutions as well as Milli-Q® water were filtered with 0.2 μm FP030/3 filters (Schleicher & Schuell GmbH, Germany). Incubations were carried out at 37 °C for 24 h.

Samples were prepared by placing a drop of DNA solution or DNA-compound solution onto mica (TED PELLA, INC. California, USA). After adsorption for five minutes at room temperature, the samples were rinsed for 10 s in a jet of deionised water (18 $M\Omega cm^{-1}$ from a Milli-Q® water purification system) directed onto the surface. The samples were blow dried with compressed argon and then imaged by AFM.

The samples were imaged using a Nanoscope III Multimode AFM (Digital Instrumentals Inc., Santa Barbara, CA) operating in tapping mode in air at a scan rate of 1–3 Hz. The AFM probe was 125 mm-long monocrystalline silicon cantilever with integrated conical shaped Si tips (Nanosensors GmbH Germany) with an average resonance frequency f_o = 330 kHz and spring constant K = 50 N/m. The cantilever was rectangular and the tip radius given by the supplier was 10 nm, a cone angle of 35° and high aspect ratio. The images were obtained at room temperature ($T = 23 \pm 2$ °C) and the relative humidity was usually lower than 40% [30].

3. Results and discussion

Four complexes of vanadium or gallium with the selected NNO ligands HL1 and HL2 (Fig. 1) were synthesized with good purity and reasonable yields. All the vanadium compounds are non conducting compounds in DMSO. The Ga(III) complex shows the molar conductivity expected for a 1:1 electrolyte [44]. Analytical and spectroscopic results are in agreement with the formulations proposed for the metal complexes: $[V^{V}O_2(L)]$, $[V^{IV}O(L1\text{-}H)(phen)]$ and $[Ga^{III}(L2)_2](NO_3)$. The proposed structural formulae are depicted in Fig. 2.

3.1. IR spectroscopic results

Some selected IR bands and their tentative assignments based on previous calculations on related vanadium compounds are included in Table 1 [47].

In the case of the $[V^{V}O_2(L)]$ complexes, the shift of the ν(C=N) band and the bands of the heterocyclic portion of the ligands, together with the non-observation of the ν(OH) vibration are in agreement with tridentate coordination of L1 and L2 through the heterocyclic nitrogen, the azomethine nitrogen ($N_{azomethine}$) and the phenolic oxygen ($O_{phenolate}$), and with the deprotonation of the ligands at the phenolic hydroxyl group. $[V^{IV}O(L1\text{-}H)(phen)]$ shows a similar spectroscopic behavior, with confirmation of the deprotonation of the NH group by the non-observation of the NH stretching band upon complexation. In this case, L1 acts as double deprotonated tridentate ligand. FTIR spectroscopic results confirmed the presence of the phenanthroline ligand in the coordination sphere of vanadium. Several bands corresponding to stretching and deformation vibrations of the heterocyclic ligands were observed in the 1700–1300 cm^{-1} region. In general, most of these bands are slightly displaced to higher frequencies upon coordination; such a feature is a typical spectroscopic behavior for phenanthroline complexes [31,48]. In addition, the $[V^{V}O_2(L)]$ complexes show two bands assigned to the symmetric and antisymmetric stretching that are characteristic of the VO_2^+ moiety. $[V^{IV}O(L1\text{-}H)(phen)]$ shows a characteristic intense band at 962 cm^{-1} assigned to ν(V=O). $[Ga(L2)_2](NO_3)$ shows a similar spectroscopic behavior to that of $[V^{V}O_2(L2)]$. New bands due to the presence of the NO_3^- are also observed.

3.2. ^{1}H NMR results for the $[V^{V}O_2(L)]$ complexes **1–2** and $[Ga^{III}(L2)_2](NO_3)$,**4**

^{1}H NMR spectroscopic data show narrow signals, typical of diamagnetic complexes. COSY experiments allowed the assignment of all ^{1}H signals for the studied complexes. ^{1}H NMR integrations and signal multiplicities are in agreement with the proposed molecular formulae. Complexation leads to shifts of the ligandś signals (Table 2). The protons placed near the coordination site show the highest signal displacements, due to the effect of the metal centre (H^6 and H^7 for $[V^{V}O_2(L1)]$ and H^1, H^5 and H^6 for HL2 complexes). The signal of the OH proton of the ligands (H^{10} for HL2 and H^1 for HL1) is not observed in the ^{1}H NMR spectra of $[V^{V}O_2(L)]$ and $[Ga^{III}(L2)_2](NO_3)$ complexes, in agreement with ligand deprotonation upon coordination.

3.3. Stability studies for $[Ga^{III}(L2)_2](NO_3)$

The stability of the complex in DMSO solution was studied by conductivity measurements during at least one week. Conductivity did not change during this period. In addition, liberation of free ligand was not detected by ^{1}H-NMR in DMSO-d_6 during at least 24 h at 30 °C.

Moreover, the stability of a 4×10^{-5} M solution of the complex in a solvent consisting of 50:50 v/v buffer PBS pH 7.0: DMSO was studied by UV–Vis spectroscopy at RT during 5 days. For this purpose the absorbance at both absorption bands of the complex (namely 459 and 440 nm), which are not present in the free ligand was followed in time. A moderate decrease of the absorbance was observed: *ca.* 9% after 24 h, 13% after 48 h and 45% after 96 h.

The complex shows very good stability in DMSO and moderate stability in aqueous – DMSO medium. Although we expect that the ligand remains bound to the metal in a high percentage when interacting with tumor and parasite cells, to assure or at least to suggest the nature of the bioactive species in complex biological medium additional studies, outside the scope of this work, would be needed.

3.4. ^{51}V NMR results for the $[V^{V}O_2(L)]$ complexes **1–2**

Solutions of both compounds were studied by ^{51}V NMR spectroscopy. For this purpose, 3 mM solutions were prepared in DMF and DMSO and kept at room temperature in contact with air. NMR spectra were measured immediately after dissolution and after a week. Results are depicted in Table 3. $[V^{V}O_2(L2)]$ shows very high stability in both solvents, since no changes were observed over a week; a single resonance is present at *ca.* −550 ppm in both solvents. The peak observed in DMSO is broader, due to the higher viscosity of this solvent. $[V^{V}O_2(L1)]$ is quite stable in DMSO; however changes are observed in DMF. The initial

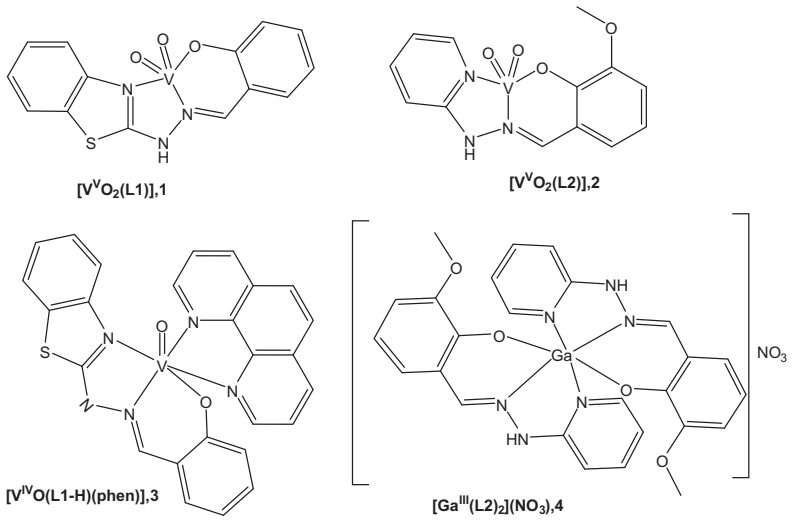

Fig. 2. Proposed molecular formulae for the new complexes obtained from the ligands HL1 and HL2.

Table 1
Tentative assignment of selected IR bands (in cm^{-1}) of the ligands and the complexes.

Compound	$\nu(VO_2)_s$	$\nu(VO_2)_{as}$	ν(VO)	ν(N=N)	ν(C=N)	ν(N–H)	ν(O–H)
L1	-	-	-	1150	1539	3037	3421
$[V^{V}O_2(L1)]$, **1**	917	973	-	1153	1547	3288	-
$[V^{IV}O(L1\text{-}H)(phen)]$, **3**	-	-	962	1153	1550	-	-
L2	-	-	-	1148	1540	3187	3458
$[V^{V}O_2(L2)]$, **2**	895	946	-	1145	1552	3191	-
$[Ga(L2)_2](NO_3)$, **4**	-	-	-	1147	1549	3192	-

Table 2
^{1}H NMR chemical shifts (δ, ppm) of $[V^{V}O_2(L)]$ and $[Ga^{III}(L2)_2](NO_3)$ complexes in DMSO-d_6 at 30 °C.

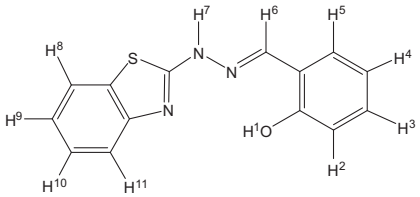

H	HL1	$[V^{V}O_2(L1)]$
1	12.20	-
2	6.93	6.80
3	7.12	7.28
4	6.93	6.80
5	7.29	7.35
6	8.46	8.68
7	10.35	not observed
8	7.64	7.53
9	7.29	7.03
10	7.29	7.28
11	7.77	7.78

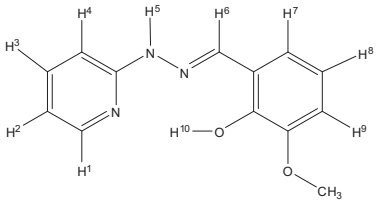

H	HL2	$[V^{V}O_2(L2)]$	$[Ga(L2)_2](NO_3)$
1	8.13	7.69	7.74
2	6.77	6.88	7.02
3	7.65	7.22	7.81
4	7.07	6.67	6.86
5	9.96	8.57	
6	8.30	8.18	8.64
7	7.22	7.13	7.02
8	6.78	6.79	6.62
9	6.95	7.01	6.86
10	10.92	-	-
CH_3	3.80	3.77	3.49

Table 3
^{51}V NMR characterization of the vanadium complexes.

Complex	Solvent	δ/ppm (t = 0)	δ/ppm (t = 1 week)
$[V^{V}O_2(L1)]$	DMF	−568 (90%)	−568 (50%)[a]
		−531 (10%)[a]	−561 (45%)
			−526 (5%)[a]
	DMSO	−564 (100%)	−560 (100%)
$[V^{V}O_2(L2)]$	DMF	−552 (100%)	−552 (100%)
	DMSO	−551 (100%)	−550 (100%)
$[V^{IV}O(L1\text{-}H)(phen)]$	DMF	−561 (100%)[b]	−561 (100%)
	DMSO	−561 (100%)[b]	−561 (100%)

[a] Broad peak.
[b] Very weak.

spectrum shows the presence of two resonances, one of them attributed to the $[V^{V}O_2(L1)]$ complex (at −568 ppm) and a broad one which may be due to oligomeric inorganic vanadates (at *ca.* −532 ppm). After a week, besides the peak of the oligomer (weaker), two other resonances are present, one broad and the other thin, *ca.* 50% each (see Fig. 3). The binding of a solvent molecule to the V^{V}-L1 compound, accompanied or not by protonation of one of the O_{oxido} donors, may affect the peak positions significantly [47]. Thus, the new peak at −561 ppm may correspond to e.g. $V^{V}O_2$(-L1)(DMF) or $V^{V}O(OH)(L1)(DMF)$, but we cannot give definite assignments for it.

3.5. EPR characterization and ^{51}V NMR results of the $[V^{IV}O(L1\text{-}H)(phen)]$ complex, **3**

The EPR spectrum of $[V^{IV}O(L1\text{-}H)(phen)]$ exhibits a hyperfine pattern consistent with axial-type spectra of monomeric $V^{IV}O$-bound species with d^{1}_{xy} ground-state configuration. Fig. 4 shows the spectra (at 77 K) obtained with 3 mM solutions of the complex in DMF and DMSO, immediately after dissolution and after one week.

The spin Hamiltonian parameters were obtained by simulation of the spectra and are approximately the same in both solvents: $g_{x,y} = 1.982$, $g_z = 1.955$, $A_{x,y} = 54.5 \times 10^{-4}\ cm^{-1}$ and $A_z = 157.0 - \times 10^{-4}\ cm^{-1}$ [49,50]. Considering the similar A_z values obtained for the previously reported $V^{IV}O$-semicarbazone phen complexes [30] and $[V^{IV}O(L1\text{-}H)(phen)]$, a similar binding set is expected, *i.e.* L1-H acting as a tridentate ligand, binding with the N,N,O donor atoms in the equatorial plane and phen binding as a bidentate ligand through the two N donors, one N in the equatorial position and the other *trans* to the oxo oxygen donor. This axial-equatorial binding geometry is frequently found in $[V^{IV}O(L\text{-tridentate})(NN)]$ complexes, where NN is bipy, phen, dppz or similar heteroaromatic ligands [51–54].

In addition, solutions of the compound in DMF and DMSO (3 mM) were also studied by ^{51}V NMR spectroscopy. The solutions were kept at room temperature in contact with air and the spectra

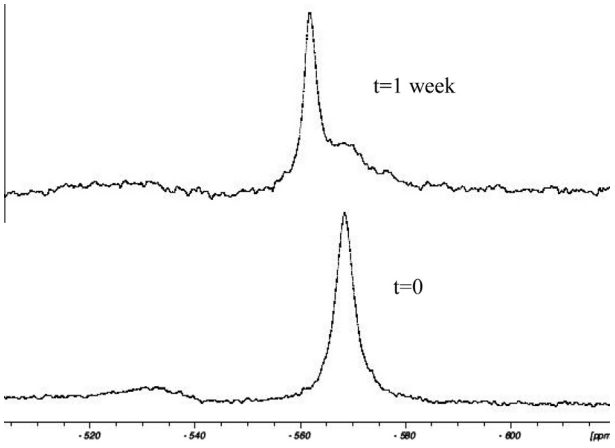

Fig. 3. ^{51}V NMR spectra of $[V^{V}O_2(L1)]$ dissolved in DMF.

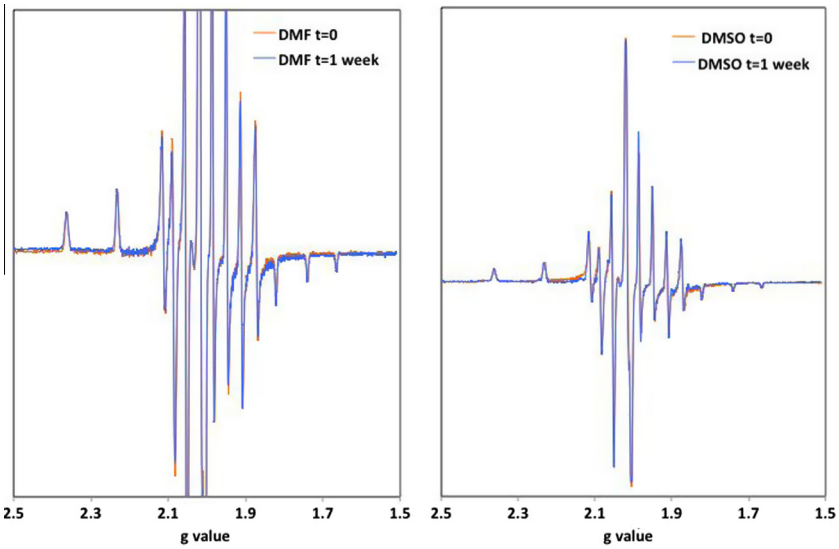

Fig. 4. 1st derivative EPR spectra of frozen solutions (77 K) of [$V^{IV}O$(L1-H)(phen)] (*ca.* 3 mM) in DMF and DMSO, after dissolution and after one week under aerobic conditions.

were measured immediately after dissolution and after a week. Results are shown in Table 2. Although the EPR data suggest that no oxidation occurred (no variation is seen on the spectra intensity, which were measured with the same acquisition parameters), analysis of the solutions by ^{51}V NMR showed that a very small amount of the complex oxidized, since a peak is observed at *ca.* −561 ppm. This initially very weak resonance in both solvents increased its intensity considerably after a week. The chemical shift is very similar to that observed for the [$V^{V}O_2$(L)] compounds, thus, suggesting that the oxidation involves the loss of the phenanthroline moiety. All peaks are in the expected range for monomeric V^{V} complexes involving N,O ligands [47,55].

Thus, it can be concluded that [$V^{IV}O$(L1-H)(phen)] shows very good stability in both organic solvents. Although presenting some oxidation after a week, the EPR characterization showed that most of it is still in the +4 oxidation state.

3.6. Biological results

3.6.1. Cell viability assays in human tumor cell lines

The cytotoxic activity of the new ligands and the respective complexes was evaluated in human cancer cells within the concentration range 0.1–200 μM after 72 h incubation and using the colorimetric MTT assay to measure the viability of the cells. For this purpose, three different human tumor cell lines were selected: the ovarian A2780, breast MCF7 and prostate PC3 cells, taking into consideration their different degrees of resistance to metallodrugs, in particular to cisplatin, which was also included in this study for comparison. A plot of the percentage of cell viability as a function of the compound concentration allowed the determination of the corresponding IC_{50} values.

All the tested compounds evidenced antiproliferative activity in the micromolar range. However, in molar units the highest cytotoxic activity was observed with [$Ga^{III}(L2)_2$](NO_3) (IC_{50}, 1.7 μM) and [$V^{IV}O$(L1-H)(phen)] (IC_{50}, 2.7 μM) against the ovarian cancer cells (Table 4 and Fig. 5). The values found for HL1 and HL2 revealed that these ligands are cytotoxic (Table 4). With the exception of [$V^{V}O_2$(L1)], the cytotoxic activity of the ligands and complexes is similar to that of cisplatin in A2780 cells and surpass cisplatin in the other tumor cell lines.

Coordination to metal ions can lead to important changes in bioactivity. Indeed, the coordination of doubly deprotonated L1-H generating the mixed-ligand complex [$V^{IV}O$(L1-H)(phen)] and of L2 to Ga^{III} lead to an increase of activity on the A2780 and MCF7 cells.

3.6.2. In vitro anti-trypanosoma cruzi activity

The complexes were evaluated in vitro for their anti- *T. cruzi* activities against epimastigotes of Dm28c strain. The results were compared to that of the reference drug Nifurtimox (Table 4). The precursors [$VO(acac)_2$] and $Ga(NO_3)_3$ were not toxic against *T. cruzi* (IC_{50} > 100 μM). HL1 was not active against the parasite while HL2 showed a low IC_{50} value, though higher than that of Nifurtimox. Formation of [$V^{V}O_2$(L2)] decreased the activity of HL2. On the other hand, coordination of HL1 to VO_2^+ forming [$V^{V}O_2$(L1)] did not improve the effect but the inclusion of the DNA-intercalating phenanthroline ligand led to a very significant increase of activity. In fact, [$V^{IV}O$(L1-H)(phen)] showed a 10-fold decrease of IC_{50} with respect to HL1 reaching an IC_{50} value of the same order of that of Nifurtimox. As previously reported for other series of [$V^{IV}O$(L-H)(NN)] compounds, where NN is a polypyridyl intercalating chelator, the presence of this NN ligand could allow the interaction of the complex with DNA, this biomolecule being a potential parasite target [23,30–33]. In the current case, the presence of this coligand is

Table 4
In vitro biological activities of the ligands and complexes: cytotoxic activity measured as the half-inhibitory concentration (IC_{50}) against A2780 (ovarian), MCF-7 (breast) and PC-3 (grade IV prostate) adenocarcinoma cells and anti-*T. cruzi* activity measured as the half growth inhibitory effect (IC_{50}) on epimastigotes of the parasite.

Compound	IC_{50} (μM)			
	A2780	MCF7	PC3	T. cruzi
HL1	5.2 ± 1.7	13.9 ± 3.5	5.5 ± 1.6	120.8 ± 5.7
[$V^{V}O_2$(L1)]	32.4 ± 14.0	39.0 ± 13.0	19.7 ± 4.0	107.0 ± 32.0
[$V^{IV}O$(L1-H)(phen)]	2.6 ± 1.2	6.2 ± 1.8	13.3 ± 3.7	10.7 ± 5.7
HL2	3.0 ± 1.6	4.9 ± 0.6	9.4 ± 2.9	23.5 ± 0.8
[$Ga^{III}(L2)_2$](NO_3)	1.7 ± 0.5	3.4 ± 0.8	9.3 ± 2.0	14.2 ± 5.1
[$V^{V}O_2$(L2)]	6.7 ± 1.3	18.2 ± 2.0	22.3 ± 6.7	45.1 ± 6.5
Cisplatin	2.5 ± 0.3	28.0 ± 6.0[a]	51.0 ± 7.0[a]	-
Nifurtimox	-	-	-	6.0 [30]

IC_{50} values are reported in μM (±SD). Cisplatin, the reference antitumor metallodrug in clinical use, and Nifurtimox, the reference antitrypanosomal drug, were included as positive controls.

[a] Taken from Refs. [56,57] obtained with the same experimental methodology and included here for comparison.

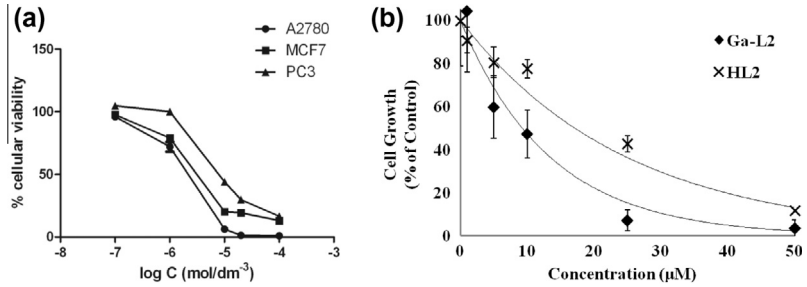

Fig. 5. (a) Dose–response curve for $[Ga^{III}(L2)_2](NO)_3$ against A2780, MCF7 and PC3 cell lines; (b) Dose - response curve on *T. cruzi* epimastigotes (Dm28c strain) for HL2 and $[Ga^{III}(L2)_2](NO)_3]$.

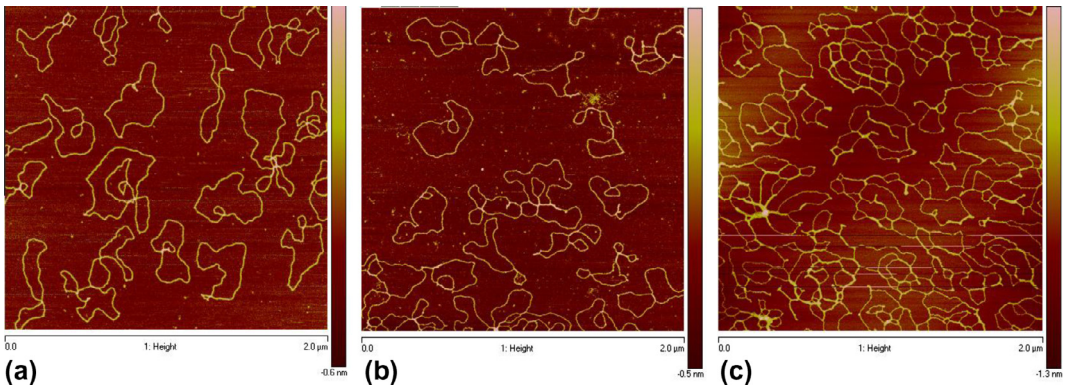

Fig. 6. AFM images showing the modifications suffered by pBR322 DNA (a) due to the interaction with $[V^{IV}O(L1\text{-}H)(phen)]$: (b) 4 h incubation at 37 °C and (c) 24 h incubation at 37 °C, for molar ratio compound: DNA base pairs 1:5.

determinant for the biological activity. On the other hand, HL2 showed significant growth inhibitory effect on the parasite. Its coordination to Ga(III) lead to a 2-fold increase in activity in molar units, but similar bioactivity if ligand molar units are considered (Table 4 and Fig. 5).

It is interesting to note that both HL1 and HL2 are cytotoxic, but their V^V-complexes, although cytotoxic, are slightly less active. This has been previously observed with other V^V-complexes on cancer cell lines and against *T. cruzi* [32]. Possibly binding to V^V decreases the amount of ligand available to produce activity or reduces permeability of cell membranes with respect to the free ligands. $[V^{IV}O(L1\text{-}H)(phen)]$ complex has proven to be quite stable to hydrolysis and to oxidation of V^{IV}, this and the presence of phen being related to its bio-activity against cancer cell lines and *T. cruzi*. In the case of $[Ga^{III}(L2)_2]^+$, although it shows increased activity, stability results suggest that the observed effect could be due to the presence in biological medium of both, the Ga complex and the free ligand.

These results globally demonstrate that coordination to V^{IV} may lead to an improvement of the antitrypanosomal activity of the ligand or to the appearance of biological effects that are not observed with the free ligand. The modification of activity depends not only on the nature of the metal centre but also on its oxidation state. The inclusion of suitable coligands may help in generating or increasing the desired biological activity.

3.6.3. Atomic-force microscopy (AFM) results

AFM has proved to be a useful tool for imaging DNA and also DNA interactions with metal complexes [58,59]. As previously demonstrated for other series of $[V^{IV}O(L\text{-}H)(NN)]$ complexes, the presence of the NN DNA intercalating coligand infers DNA as a target either in the parasites or in tumor cells. In order to explain the high growth inhibitory activity of $[V^{IV}O(L1\text{-}H)(phen)]$, the interaction of this compound with DNA was preliminarily studied by AFM using pBR322 plasmid as a model molecule. AFM images are depicted in Fig. 6. The complex modified the tertiary structure of the plasmid. This is visualized as changes in the DNA shape. These observations thus indicate that the compound interacts with DNA but more studies involving other techniques are needed to clearly establish DNA as the main target to explain its cytotoxicity.

4. Conclusions

New vanadium and gallium complexes of NNO ligands HL1 and HL2 were synthesized with high purity and good yields. The compounds were fully characterized in the solid state and in solution by using different techniques. The stability with time of the compounds in solution was studied. Their anti- *T. cruzi* activities, assessed on Dm28c epimastigotes, showed that the most potent inhibitors were HL2, $[Ga^{III}(L2)_2](NO_3)$ and $[V^{IV}O(L1\text{-}H)(phen)]$. Remarkably, these compounds present a considerably high cytotoxicity in the ovarian cancer cell lines, indicating a correlation between antitrypanosomal and antitumor activities.

Furthermore, although additional studies are required, this set of results suggests that the tested ligands may be considered as leading compounds for a new generation of antitrypanosomal compounds also possessing anticancer properties.

Acknowledgements

I.M. and M.F. thank Agencia Nacional de Investigación e Innovación (ANII, Uruguay) for their research grants. Authors would like

to thank RIIDFCM (209RT0380) CYTED network for supporting collaborative research on development of bioactive metal-based compounds, and also the financial support of Fundação para a Ciência e Tecnologia (FCT, Portugal), PEst-OE/QUI/UI0100/2013, PTDC/QUI-QUI/119561/2010 and CIÊNCIA2007, and the Portuguese NMR and Mass Spectrometry Networks (IST-UTL Centers) and ICREA (Institució Catalana de Recerca i Estudis Avançats) and Ministerio de Economía y Competitividad de España (Proyecto CTQ2011-27929-C02-01). P.G. acknowledges the support of COST Actions CM1003 and CM1105.

References

[1] (a) The World Health Organization website retrieved on March, 2013, http://www.who.int/mediacentre/factsheets/fs297/en/index.html.; (b) SEER Cancer Statistics, U.S. National Cancer Institute website, http://seer.cancer.gov/statfacts/html/all.html retrieved on March, 2013.
[2] P.C. Bruijnincx, P.J. Sadler, Curr. Opin. Chem. Biol. 12 (2008) 197.
[3] T.W. Hambley, Dalton Trans. (2007) 4929.
[4] L. Ronconi, P.J. Sadler, Coord. Chem. Rev. 251 (2007) 1633.
[5] K.H. Thompson, C. Orvig, Dalton Trans. (2006) 761.
[6] M.A. Jakupec, M.V. Galanski, B. Arion, C.G. Hartinger, B.K. Keppler, Dalton Trans. (2008) 183.
[7] S.H. van Rijt, P.J. Sadler, Drug Discov. Today 14 (2009) 1089.
[8] P.J. Dyson, G. Sava, Dalton Trans. (2006) 1929.
[9] E.J. Baran, Lat. Am. J. Pharm. 27 (2008) 776.
[10] T. Gianferrara, I. Bratsos, E. Alessio, Dalton Trans. (2009) 7588.
[11] M.A. Jakupec, B.K. Keppler, Curr. Top. Med. Chem. 4 (2004) 1575.
[12] M. Jakupec, B.K. Keppler, in: A. Sigel, H. Sigel (Eds.), Metal Ions in Biological Systems, Vol. 42, Marcel Dekker, New York, 2004, p. 425.
[13] M. Chua, L.R. Bernstein, R. Li, S.K.S. So, Anticancer Res. 26 (2006) 1739.
[14] F. Silva, F. Marques, I.C. Santos, A. Paulo, A.S. Rodrigues, J. Rueff, I. Santos, J. Inorg. Biochem. 104 (2010) 523.
[15] D. Rehder, Bioinorganic Vanadium Chemistry, John Wiley & Sons, Chichester, 2008.
[16] D. Rehder, Med. Chem. 4 (2012) 1823.
[17] G.R. Willsky, L.H. Chi, M. Godzala, P.J. Kostyniak, J.J. Smee, A.M. Trujillo, J.A. Alfano, W.J. Ding, Z.H. Hu, D.C. Crans, Coord. Chem. Rev. 255 (2011) 2258.
[18] A.M. Evangelou, Crit. Rev. Oncol. Hematol. 42 (2002) 249.
[19] I. Ribeiro, A.M. Sevcsik, F. Alves, G. Diap, R. Don, M.O. Harhay, S. Chang, B. Pecoul, PLoS. Negl. Trop. Dis. 3 (2009) e484, http://dx.doi.org/10.1371/journal.pntd.0000484.
[20] J.D. Maya, B.K. Cassels, P. Iturriaga-Vásquez, J. Ferreira, M. Faúndez, N. Galanti, A. Ferreira, A. Morello, Comp. Biochem. Physiol. A 146 (2007) 601.
[21] J.A. Urbina, Drugs Future 35 (2010) 409.
[22] R.A. Sánchez-Delgado, A. Anzellotti, L. Suárez, Metal ions in Biological Systems, in: H. Sigel, A. Sigel (Eds.), Metal Ions and Their Complexes in Medication, Vol. 4, Marcel Dekker, New York, 2004, p. 379.
[23] D. Gambino, Coord. Chem. Rev. 255 (2011) 2193.
[24] D.R. Magalhães Moreira, A.C. Lima Leite, R. Ribeiro dos Santos, M.B.P. Soares, Curr. Drug Targets 10 (2009) 212.
[25] A. Cavalli, M.L. Bolognesi, J. Med. Chem. 52 (2009) 7339.
[26] S.P. Fricker, R.M. Mosi, B.R. Cameron, I. Baird, Y. Zhu, V. Anastassov, J. Cox, P.S. Doyle, E. Hansell, G. Lau, J. Langille, M. Olsen, L. Qin, R. Skerlj, R.S.Y. Wong, Z. Santucci, J.H. McKerrow, J. Inorg. Biochem. 102 (2008) 1839.
[27] D. Gambino, L. Otero, Inorg. Chim. Acta 393 (2012) 103.
[28] M. Navarro, G. Gabbiani, L. Messori, D. Gambino, Drug Discov. Today 15 (2010) 1070.
[29] K. Kinnamon, E.A. Steck, E.S. Rane, Antimicrob. Agents Chemother. 15 (1979) 157.
[30] J. Benítez, L. Becco, I. Correia, S. Milena, J. Inorg. Biochem. 105 (2011) 303.
[31] J. Benítez, I. Correia, L. Becco, M. Fernández, B. Garat, H. Gallardo, G. Conte, M.L. Kuznetsov, A. Neves, V. Moreno, J. Costa, Z. Anorg. Allg. Chem. 639 (2013) 1417.
[32] M. Fernández, L. Becco, I. Correia, J. Benítez, O. E. Piro, G. A. Echeverria, A. Medeiros, M. Comini, M. L. Lavaggi, M. González, H. Cerecetto, V. Moreno, J. Costa, Pessoa, B. Garat, D. Gambino, J. Inorg. Biochem. 10.1016/j.jinorgbio.2013.02.010.
[33] J. Benítez, A. Cavalcanti de Queiroz, I. Correia, M. Amaral, Eur. J. Med. Chem. 62 (2013) 20.
[34] D. Gambino, M. Fernández, D. Santos, G.A. Etcheverría, O.E. Piro, F.R. Pavan, C.Q.F. Leite, I. Tomaz, F. Marques, Polyhedron 30 (2011) 1360.
[35] B. Demoro, M. Rossi, F. Caruso, D. Liebowitz, C. Olea-Azar, U. Kemmerling, J.D. Maya, H. Guiset, V. Moreno, C. Pizzo, G. Mahler, L. Otero, D. Gambino, Biol. Trace Elem. Res. 153 (2013) 371.
[36] B. Demoro, R.F.M. de Almeida, F. Marques, C.P. Matos, L. Otero, J. Costa, Dalton Trans. 42 (2013) 7131.
[37] D. Santos, B. Parajón, J. Inorg. Biochem. 117 (2012) 270.
[38] N. Gómez, D. Santos, R. Vázquez, L. Suescun, Á. Mombrú, M. Vermeulen, L. Finkielsztein, C. Shayo, A. Moglioni, D. Gambino, C. Davio, ChemMedChem 6 (2011) 1485.
[39] L. Becco, A. Rodríguez, M. Elena, J. Inorg. Biochem. 109 (2012) 49.
[40] M. Mohan, N.S. Gupta, L. Chandra, N.K. Jha, R.S. Prasad, Inorg. Chim. Acta 141 (1988) 185.
[41] J. Tang, J.S. Costa, S. Smulders, G. Molnár, A. Bousseksou, S.J. Teat, Y. Li, G.A. van Albada, P. Gamez, J. Reedijk, Inorg. Chem. 48 (2009) 2128.
[42] J. Tang, J.S. Costa, G. Aromí, I. Mutikainen, U. Turpeinen, P. Gamez, J. Reedijk, Eur. J. Inorg. Chem. (2007) 4119.
[43] Y. Gao, Y. Ji, S. Ding, Z. Liu, J. Tang, Z. Anorg, Allerg. Chem. 637 (2011) 2300.
[44] J. Geary, Coord. Chem. Rev. 7 (1971) 81.
[45] A. Rockenbauer, L. Korecz, Appl. Magn. Reson. 10 (1996) 29.
[46] T. Mosmann, J. Immunol. Methods 65 (1983) 55.
[47] M.R. Maurya, C. Haldar, A. Kumar, M.L. Kuznetsov, F. Avecilla, J. Costa Pessoa, Dalton Trans. 42 (2013) 11941.
[48] I.E. León, S.B. Etcheverry, B.S. Parajón-Costa, E.J. Baran, Biol. Trace Elem. Res. 147 (2012) 403.
[49] K. Wüthrich, Helv. Chim. Acta 48 (1965) 1012.
[50] N.D. Chasteen, in: J. Lawrence, L. Berliner, J. Reuben (Eds.), Biological Magnetic Resonance, vol. 3, Plenum Press, New York, 1981, p. 53.
[51] I. Cavaco, J. Costa, J. Chem. Soc., Dalton Trans. (1994) 149.
[52] J. Costa Pessoa, M.J. Calhorda, I. Cavaco, I. Correia, M.T. Duarte, V. Felix, R.T. Henriques, M.F.M. Piedade, I. Tomaz, J. Chem. Soc., Dalton Trans. (2002) 4407.
[53] I. Cavaco, J. Costa, J. Chem. Soc., Dalton Trans. (1996) 1989.
[54] J. Costa Pessoa, I. Cavaco, I. Correia, M.T. Duarte, R.D. Gillard, R.T. Henriques, F.J. Higes, C. Madeira, I. Tomaz, Inorg. Chim. Acta 293 (1999) 1.
[55] M.R. Maurya, A.A. Khan, A. Azam, S. Ranjan, N. Mondal, A. Kumar, F. Avecilla, J. Costa Pessoa, Dalton Trans. 39 (2010) 1345.
[56] B. Demoro, R.F.M. de Almeida, F. Marques, C.P. Matos, L. Otero, J. Costa, Dalton Trans. 42 (2013) 731.
[57] S. Gama, F. Mendes, F. Marques, I.C. Santos, M.F. Carvalho, I. Correia, J. Costa, J. Inorg. Biochem. 105 (2011) 637.
[58] G.B. Onoa, G. Cervantes, V. Moreno, M.J. Prieto, Nucleic Acids Res. 26 (1998) 1473.
[59] M. Vieites, P. Smircich, M. Pagano, L. Otero, F. Luane, J. Inorg. Biochem. 105 (2011) 1704.